Band structures, gap states and doping effects in amorphous hydrogenated and crystalline silicon studied by soft X-ray emission

1991 J. Phys.: Condens. Matter 3 9637

(http://iopscience.iop.org/0953-8984/3/48/006)

J. Phys.: Condens. Matter 3 (1991) 9637–9650. Printed in the UK

Band structures, gap states and doping effects in amorphous hydrogenated and crystalline silicon studied by soft x-ray emission

R S Crisp† and D Haneman‡

† Department of Physics, The University of Western Australia, Nedlands, WA 6009, Australia

‡ School of Physics, University of New South Wales, POB 1, Kensington, Australia 2033

Received 19 June 1991, in final form 2 September 1991

Abstract. The soft x-ray L_{23} emission spectra for various hydrogenated amorphous silicon (ASIL) and crystalline silicon samples have been analysed. The significant differences in the valence band structure for p-type compared with n- and i-type ASIL films are ascribed to greater structural disorder in the former. The presence of apparent high densities of states in the ASIL energy gap region is ascribed to cross transitions from nearest-neighbour hydrogen states to shifted core states of silicon. Both B and P dopant atoms have been directly detected from their emission spectra. Comparison of results for ASIL films made with 1% and 20% phosphine-in-silane show a gas atom incorporation ratio that is seven times higher for the 20% film.

1. Introduction

Soft x-ray emission spectroscopy (SXS) is an established technique for deriving information about the density of valence band states in solids, as well as inner levels. Recent measurements (Senemaud *et al* 1982, Terekhov *et al* 1984, 1986, Crisp *et al* 1988) of the valence band for amorphous hydrogenated silicon (ASIL) films have shown the presence of a significant density of states above the valence band edge which were interpreted (Senemaud *et al* 1982, Terekhov *et al* 1986) as the well-known energy gap states of ASIL. However, it has been shown (Crisp *et al* 1988) that this could not generally be so since the observed densities were two orders of magnitude higher than the known gap state densities. To compound the problem it was found that states were observable above the valence band edge even for some crystalline silicon samples (Crisp *et al* 1988), where there are no gap states. In the latter case, it was proposed that the emission was due to states at the interface between the silicon surface oxide layer and a layer of contaminant. Since the ASIL 'gap state' emission was only about double that of crystalline Si, it was tentatively suggested that a similar explanation might also be applicable for this material, namely surface contamination effects (Crisp *et al* 1988).

This latter suggestion does not accord well with some data in the literature, and with further data obtained by us and reported here. We will propose what we regard as a better explanation which involves shifted core states. We have also studied the

0953-8984/91/489637+14$03.50

valence bands of variously doped films and, in particular, heavily doped films where we directly detected the valence emission from phosphorus and boron dopants. Valence band effects from doping will be discussed.

2. Experimental details

The specimens were specially shaped blocks of single and polycrystal silicon, given various polishing and etching treatments, and similarly shaped blocks of pure copper on which ASIL films were deposited by the usual RF discharge-in-silane (plasma-assisted CVD) process. Doped films were produced using phosphine in 1% or 20% ratio to silane (heavy doping), or a diborane-in-silane mixture of $\frac{3}{4}$% diborane. This cylinder reservoir was several years old and it is believed that the diborane decomposes in less than this time. Nonetheless, p-type films were formed with conductivities of 1×10^{-5} $(\Omega\ \mathrm{cm})^{-1}$ and the incorporation of boron from such 'old' gas sources was shown by detection of the boron K emission as described later.

The ASIL samples were stored, soon after production, in sealed vacuum ampoules which were opened just before insertion of the samples into the vacuum spectrometer. The targets were cooled with liquid nitrogen. Electron beam currents of 1.0 to 3.0 mA at 3.5 kV (unless otherwise stated) were used to excite spectra. With efficient cold trapping, and a working pressure of less than 5×10^{-8} Torr, sample contamination was slight.

The 1 m spectrometer uses a grating ruled in gold with 2400 grooves mm^{-1} and a 1° blaze, which is mounted at 85.5° (4.5° grazing angle). Photoelectric detection is by means of an EMI type 9642/2B 18 stage electron multiplier with a 3000 Å layer of CsI evaporated onto the first dynode to enhance the quantum efficiency. The instrument operates in a scanning mode, with several scans lasting a total of 30 min or more, being summed to give the final spectrum. Data are collected in real time into a Digital Systems LSI 11/23 computer.

The optical resolution, set by the 45 μm entrance and analysing slits and the grating parameters, is 0.25 Å to first order, with no loss in resolution due to the finite channel widths generated by the computer (typically ten or more channels across the optical window). No correction for instrumental width was necessary.

When comparing the intensities of the features, the spectra should be normalized to equal areas under the Si-L_{23} band profiles. However, for display purposes, it is convenient to normalize spectra to the maximum intensities. The procedure used is indicated in the figure captions. For clarity, the number of points plotted in the figures is about one half of the number recorded.

3. Results

3.1. Valence bands

We first consider the emission due to electrons in valence band states making transitions to holes in the L_2 and L_3 core levels in Si ($2p_{1/2}$ and $2p_{3/2}$ core states). The shape of the valence band should differ somewhat for p- and n-type ASIL due to the different dopant induced states, and it was of interest whether this would be detectable. In fact differences were noted but in order to estimate their significance it was first

necessary to assess the reliability as well as the reproducibility of the valence band data.

Transitions occur to the p-like core states; hence, to the extent that the valence states are hydrogenic, selection rules limit the final states to those with s-like (or d-like) wavefunctions. Thus in figure 1 the two lower energy peaks, at 90 and 92 eV, are ascribed to s-like states in the valence band (Kurmaev and Wiech 1985). The shape of the L_{23} band for c-Si has been calculated by Klima (1970), and the general band shape is in accord with that deduced by x-ray photoelectron spectroscopy data. There is a p-like group of states at about 95 eV near the top of the band, seen as a peak by SXS involving K (s-type) core states (Kurmaev and Wiech 1985), which is not apparent in SXS involving L (p-type) states. However, in the L_{23} spectrum there remains a prominent hump at 95 eV. In the case of ASIL, the two low-energy peaks become broadened and barely distinguishable, due presumably to distributions of bond angles and stresses spreading the s-like states, and the high-energy hump becomes somewhat less prominent, as in figure 2. However, this hump appears to be significantly higher for heavily p-type ASIL, compared with i- and n-type ASIL, figure 2.

To test the sensitivity of this portion of the valence band to structure, the band was also measured for various types of crystalline silicon, shown in figure 1. Note in figure 1(*a*), for unetched lapped surfaces, that at low exciting voltages (1.2 kV) the band shape tends towards that of ASIL in that the low-energy peaks and 95 eV hump become less prominent. Since at low voltages the surface regions contribute more to the emission, the results reflect the effect of oxides and, more particularly, the effect of surface stresses arising from mechanical polishing. Similar data were taken for etched samples, with lower surface stresses. Although the low-energy (s) peaks are now less broadened at lower exciting voltages, the 95 eV hump becomes more prominent, figures 1(*b*)–(*d*). This is particularly so in figure 1(*d*) for an etched polycrystalline surface that had been exposed to air for 3 h before insertion in the spectrometer vacuum. To confirm this point, data were taken for a polycrystalline Si sample oxidized in dry air at 850 °C for 30 h. This would have given about 150 nm of oxide. As expected the SXS data shown in figure 3 are completely different with a prominent peak at 94.5 eV. Clearly the 95 eV hump region is particularly sensitive to the surface oxide, which is less for the samples in figures 1(*b*) and (*c*) which were inserted immediately after etching. At high beam energy, the spectra in figures 1(*b*), (*c*) and (*d*) are essentially the same, confirming that bulk effects then predominate, as is known from penetration depth studies. We may note in figure 3 that the spectra from the oxide at 1 and 3 kV are similar, confirming the growth of a thick oxide layer.

We now examine the ASIL valence band spectra in figure 2. It is clear that the curves from intrinsic ASIL and also heavily doped (1% PH_3:SiH_4) and extra heavily doped (20% PH_3:SiH_4) ASIL appear to differ from that for the p-type film. The latter shows a distinctly higher and steeper hump in the 95 eV region. Such data were repeated for a number of films and the difference is reproducible. This energy region is the one that shows an increase when the incident voltage is reduced (figure 1) and, as discussed in the case of c-Si, appears to respond sensitively to departures from the normal crystal structure. We therefore interpret the ASIL data as indicating that p-type films doped with boron have more structural disorder than n-type films. Even very heavily doped n-type films are not very different from intrinsic films in the 95 eV valence band region, figure 2.

The result that the valence band structure is more affected by B doping than P doping is consistent with other studies. Yamasaki *et al* (1982) found significant

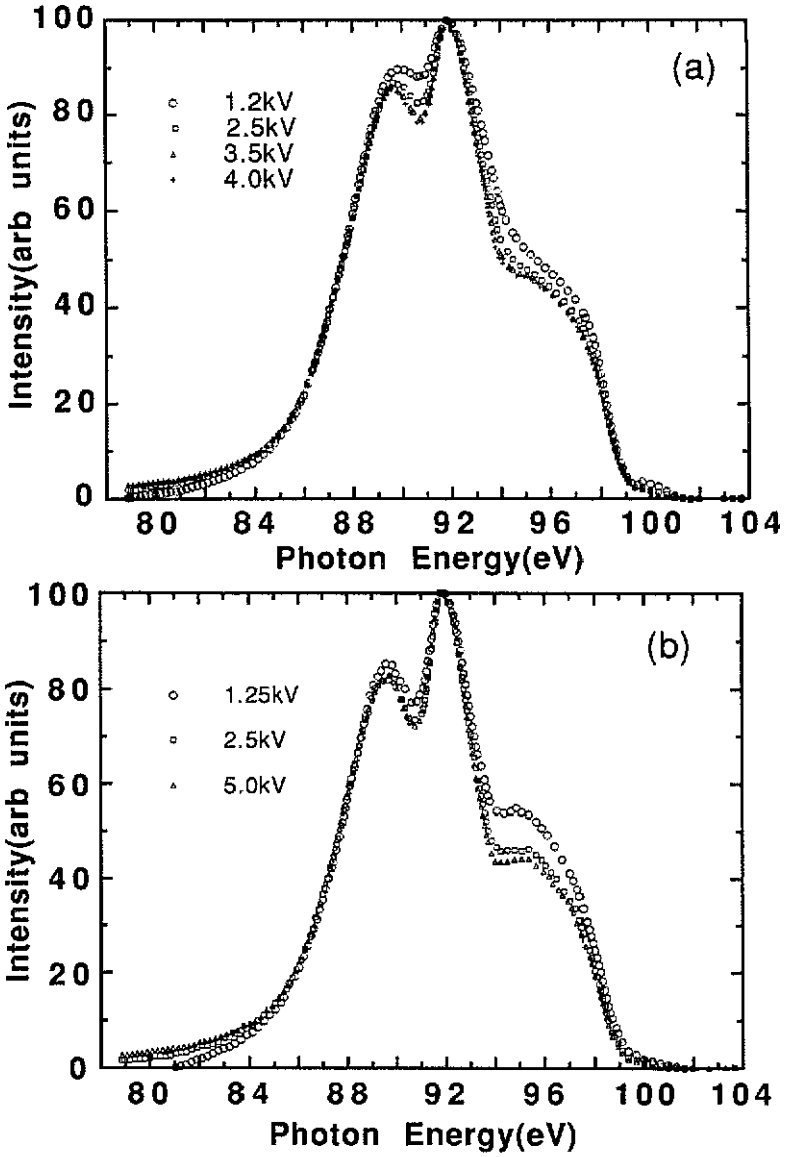

Figure 1. Si-L_{23} emission bands from c-Si recorded at various voltages: (*a*) lapped polycrystalline Si, no etching; (*b*) single crystal Si etched with HF; (*c*) polycrystalline Si lapped and etched with CP4; and (*d*) as for (*c*) followed by exposure to air for 8 h.

mechanical structure effects in films made from B_2H_6:SiH_4 gas mixtures with ratios of diborane greater than 10^{-3}. Reimer *et al* (1981) noted B clustering within heavily B doped films. The natures of B and P incorporation in ASIL are quite different as found by Ready and Boyce (1987) with nuclear magnetic resonance spin echo experiments. Whereas most P atoms do not have H as a nearest neighbour, 40% of B atoms have an H atom as a nearest neighbour at 0.16 nm, indicating direct bonding. This would explain why the valence band density of states is affected more by B than by P.

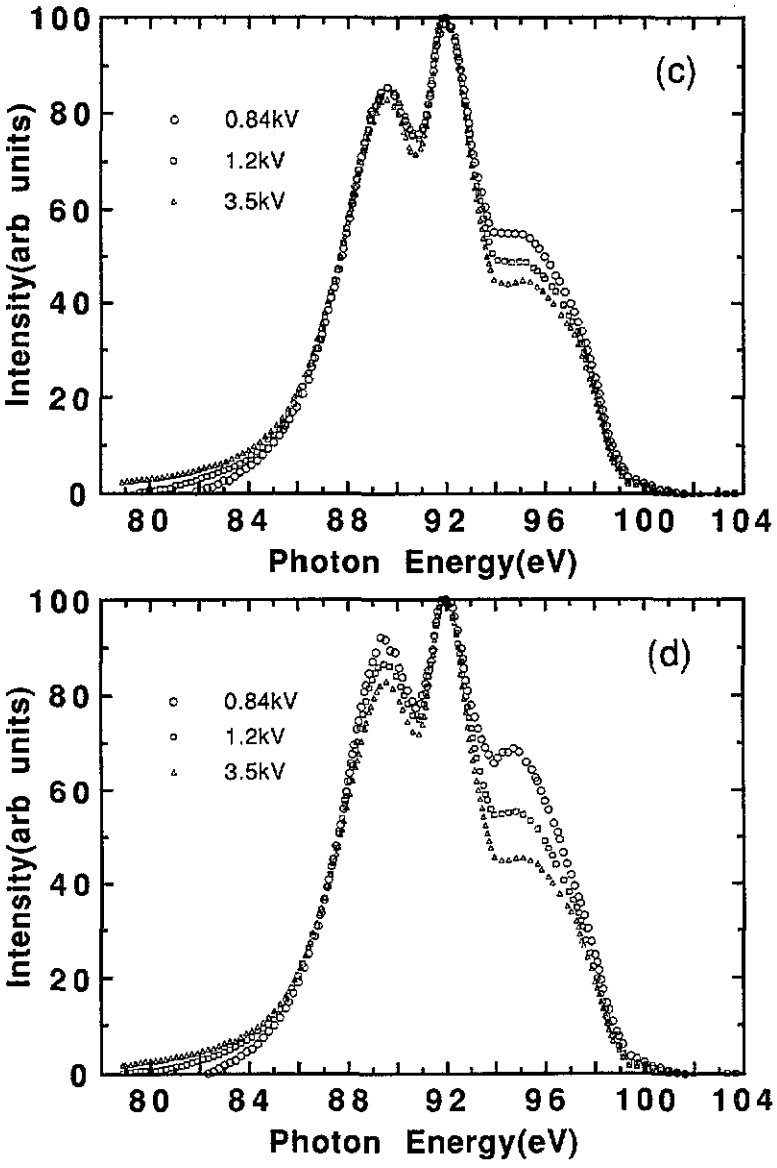

Figure 1. (Continued)

3.2. Gap state regions

Figure 4 shows data for the region of the emission above the top of the valence band E_v, the so-called gap states. Similar data for a less heavily doped sample have been previously reported by us (Crisp *et al* 1988), and similar emissions had been reported earlier by Terekhov *et al* (1986). As discussed (Crisp *et al* 1988) the integrated intensities correspond to 10^{19} states cm^{-3} eV^{-1} if distributed uniformly over the emitting zone which is approximately 400 atomic layers deep. This is some two orders of magnitude higher than the maximum gap state density in good quality ASIL at about 1 eV above E_v. If the emission is regarded as coming only from the surface region, say the first 50 layers, it corresponds to at least five times the previous density.

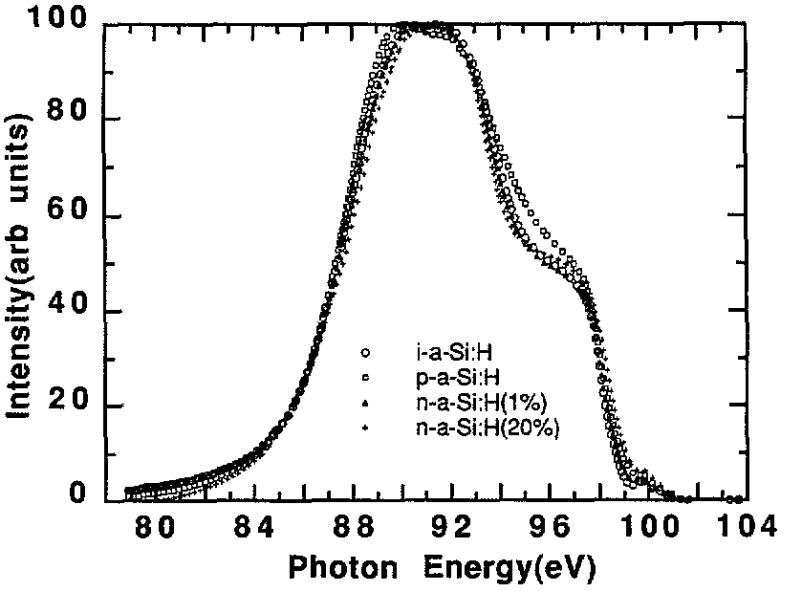

Figure 2. Si-L_{23} bands from intrinsic and both n- and p-doped a-Si:H. All recorded at 3.5 kV and normalized to the peak intensity.

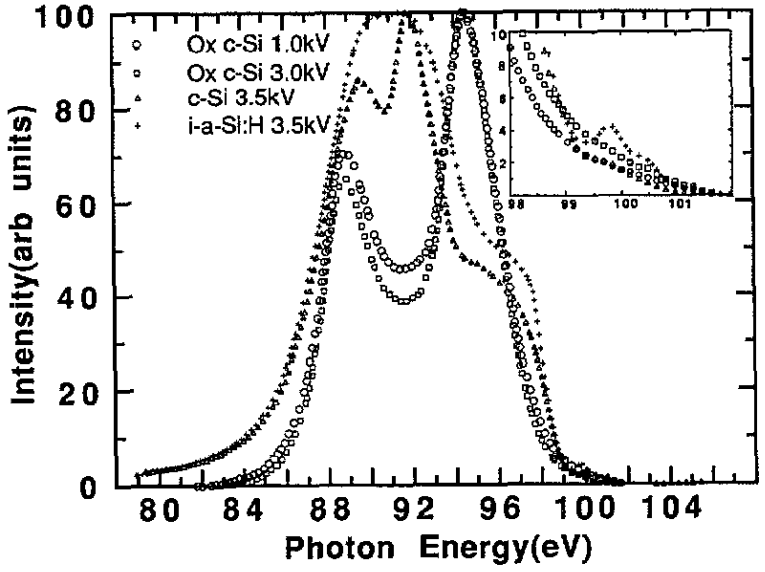

Figure 3. Si-L_{23} emission bands from oxidized polycrystalline Si with bands from polycrystalline Si and a-Si:H for comparison. The inset of the gap region on an enlarged scale shows the prominent 'gap state' emission feature appearing in amorphous material but not in either clean or oxidized c-Si. All spectra were recorded at 3.5 kV and normalized to the peak intensity.

Although the valence band high-energy tail density in the surface region could be an order of magnitude higher than in the bulk (Winer and Ley 1988), the density observed would still end up as about two orders of magnitude too high. Hence an

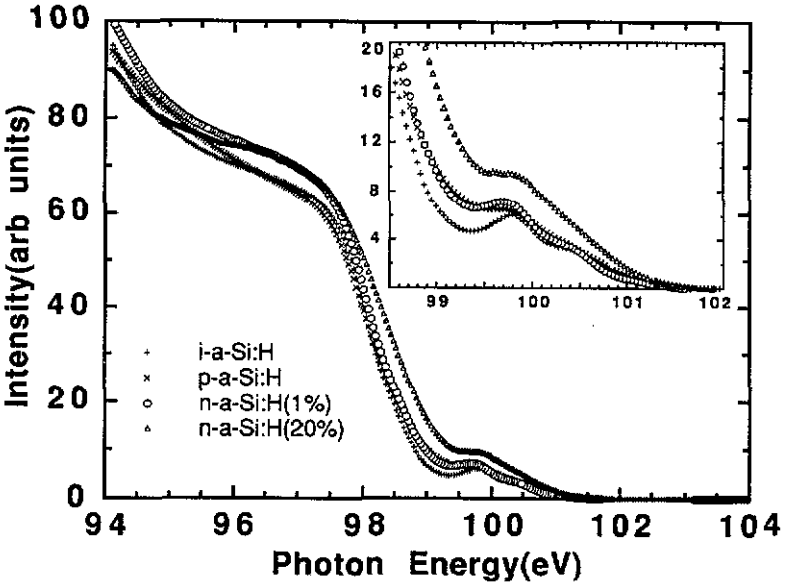

Figure 4. Gap state emission from intrinsic and doped a-Si:H, all recorded at 3.5 kV and normalized to equal areas under the main Si-L_{23} band.

explanation for the observed emission must be sought in some other way.

We refer now to data from Terekhov *et al* (1986), showing gap state emission for various ASIL samples prepared with different discharge voltages during the RF plasma deposition process. This gave films of differing hydrogen concentrations and of differing quality, measuring the latter by the ratio R of photo-to-dark conductivity (using light at 0.6 μm and 10^{18} photon cm^{-2}). This ratio R varied monotonically from 40 up to 7×10^4 for eight films and the gap state distribution varied correspondingly, the region just above E_v dropping in intensity with improving film quality until a clear dip developed at about 99.2 eV for their best film. This spectrum was similar to our data for intrinsic films, which had a light (one sun) to-dark-conductivity ratio of 10^5. Hence the data for good films are in general agreement. Furthermore, for the best films ($R > 3 \times 10^3$) in the previously mentioned series, a peak developed at about 99.8 eV, corresponding well with the peak seen in our data, figure 4.

These systematic trends do not accord well with an explanation in terms of surface contamination as the cause of the surface emission. Indeed it is believed that there is very little oxide, perhaps only a few layers on ASIL (Winer and Ley 1988) and a contaminant layer on top of that could hardly be thought to vary systematically with film quality R. Therefore we do not favour our earlier tentative suggestion of this as an explanation for the gap state emission. The evidence from the work of Terekhov *et al* (1986), and our present data for differently doped device quality films, strongly suggests that some bulk property of the films is responsible for the emission.

It has been suggested that core excitons may be responsible for the gap state emission (Carson and Schnatterly 1987). However, the differences between the results from ASIL films of different dopings are consistent, e.g. the pronounced dip at 99.2 eV for intrinsic films compared with the n and p films, see figure 4 and figure 5 of Crisp *et al* (1988); the data of Terekhov *et al*; and the even sharper dip for the intrinsic film made by reactive sputtering, shown by Carson and Schnatterly. It is difficult to understand

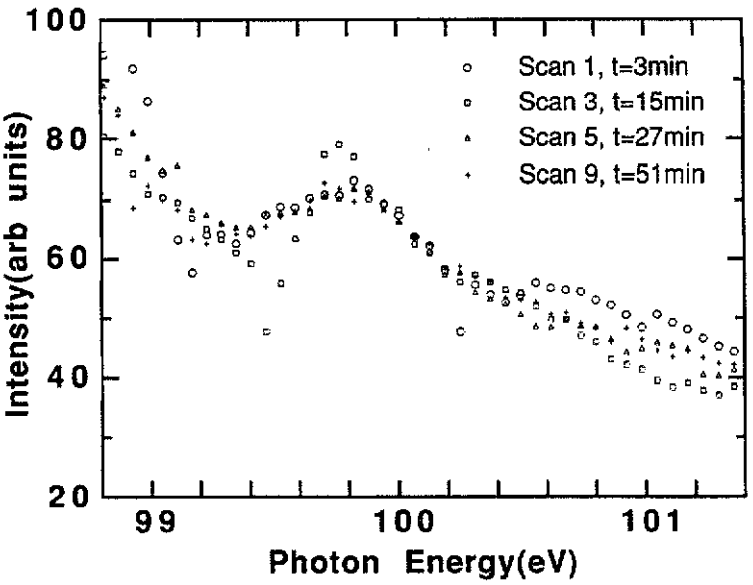

Figure 5. Four (of ten) scans recorded in succession at 3.5 kV with current reduced to 0.006 mA and a shortened scan duration of 6 min to demonstrate the absence of time dependent change in the gap state intensity. The start times of each scan are indicated relative to $t = 0$ being the instant when the beam was first switched on. Intensities are normalized to the background intensity at 101.5 eV.

why core exciton effects should differ so much in films with relatively slight dopant differences. Therefore although a small excitonic effect might be present, particularly for c-Si, we believe the true explanation for ASIL must lie with the properties of the films.

In this connection we take into account that during our SXS measurements, the target material is being subjected to relatively intense electron bombardment, typically 80 mA cm^{-2} at about 3 kV which is 240 W cm^{-2}. In crystalline materials, the energies are too low to cause significant lattice damage, but in ASIL with its various weak bond sites, it is known (see Schneider and Schröder 1988) that measurable damage occurs, to a depth of 200 nm at 3 keV, and around 10 nm at 1.1 keV. Such keV electron irradiation appears to create the same kind of completely annealable defects, namely dangling bonds, as does light soaking. After 16 min of several keV electron irradiation at 72 mW cm^{-2}, i.e. 69 J cm^{-2}, the gap density of states increased by a factor of 30, to over 10^{17} cm^{-3} eV^{-1}. After 20 keV irradiation at 100 J cm^{-2}, the gap state density was over 10^{17} cm^{-3} eV^{-1}. These data refer to irradiations which are very small compared with those in SXS. At 3 keV energy with 1.0 mA a scan is completed in 25 min for a total electron irradiation of 1.8×10^5 J cm^{-2} which is more than three orders of magnitude higher than the previous figures and would suggest that defect densities of order 10^{20} cm^{-3} eV^{-1} were possible, assuming the same kind of extrapolation occurs as at lower doses. However some saturation appears to be beginning at doses above 10^2 J cm^{-2} (see Schneider and Schröder 1988, figure 13), so that the defect density could perhaps be 10^{19} cm^{-3} eV^{-1} as observed.

To test this hypothesis, we carried out fast scans at reduced exciting currents of only 0.006 mA. The first scan was completed at 10 min after switching the beam on, with a total irradiation of 4.3×10^2 J cm^{-2}. Subsequently nine more scans were

made at 5 min intervals. Although the signal-to-noise ratio was reduced, as shown in figure 5, it was nevertheless quite clear that there was no systematic build-up in the intensity of the gap state emission. It was just as prominent in the first as in the last scan, and similar to that from high current scans. Since the incident current was reduced by a factor of at least 150 we should, on these figures, have seen a clearly reduced emission if beam-induced defect states were responsible. Thus the conclusion is that beam-induced defect states do not contribute significantly to the observed gap state emission.

As an additional check, measurements were also carried out with the sample held at annealing temperatures up to 180 °C, which would remove any supposed bombardment damage. No difference in the gap emission was observed.

We now believe that the true explanation for the high emission in the gap state region is based on the consideration of two other factors. The first is that the Si 2p core levels, which are the final states in the observed transitions, are shifted to higher binding energies when the Si atom is bonded to hydrogen. According to the measurements of Ley *et al* (1982), the shift is 340 meV per attached H atom, so that SiH_3 groups in the ASIL have a Si 2p core level shift of 1.02 eV. Transitions to these levels by the Si valence electrons would certainly cause a photon energy tail extending 1 eV beyond the normal distributions seen in the data. However, this could not explain the observed dip in the gap state distributions for high quality ASIL as in figure 4, since only an extended tail could be produced.

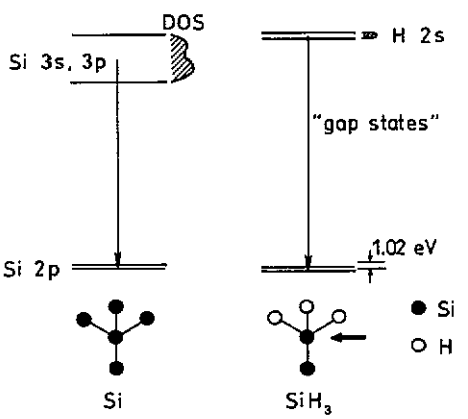

Figure 6. Schematic diagram illustrating the origin of gap state emission observed above the valence band emission limit and arising from electron transitions by electrons in H 2s states to Si-L_{23} core states which are shifted for Si atoms in SiH_3 groups.

We therefore postulate that there exists a narrow distribution of states at the top of the valence band, which is associated with the hydrogen atoms, as shown schematically in figure 6. A simple interpretation of its origin is that it is derived from H 2s states. The theoretical H 2s level for an isolated H atom is at $(13.6/4) = -3.4$ eV with respect to the vacuum level. Therefore the occurrence of either a narrow band, or distribution of localized levels, from this source in the ASIL matrix at about -4.5 to -5 eV is plausible. Indeed theoretical calculations of H-derived states in ASIL have predicted the presence of a narrow band in the energy gap region or just above it (Ching *et al* 1979, Allan and Joannopoulos 1980). This band is not seen in photoemission studies

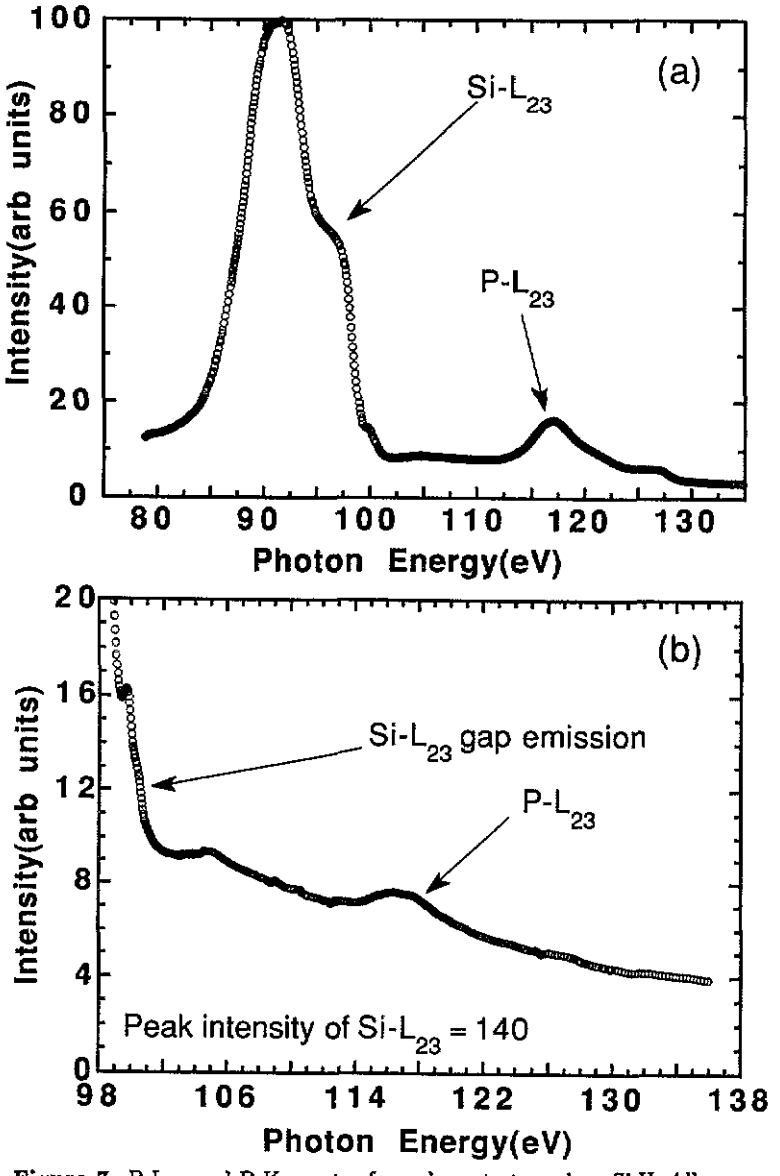

Figure 7. P-L_{23} and B-K spectra from dopant atoms in a-Si:H. All were recorded at 3.5 kV. For (*a*) to (*d*) the structure underlying the P-L_{23} component is a satellite structure of the main Si-L_{23} band. (*a*) Si-L_{23} band and P-L_{23} band for a-Si:H deposited with 20% PH_3:SiH_4 to show the relationship of the two bands and the extended Si-L_{23} satellite structure; (*b*) P-L_{23} band from 1% PH_3 sample; (*c*) P-L_{23} band from 20% PH_3 sample; and (*d*) B-K from 0.75% B_2H_6 sample also showing O-Kα in third order. The upper part of figure (*d*) shows the background and its removal.

(Ley 1984, Wesner and Eberhardt 1983), but the sensitivity of such studies is such that a band of intensity less than about 1% of the average valence emission would be hard to detect. In our case we postulate the distribution to occur as shown in figure 6, with a density of only about 10^{19} cm^{-3} eV^{-1}. This would not be directly visible in ordinary studies of ASIL states, nor in UPS measurements (which in any case

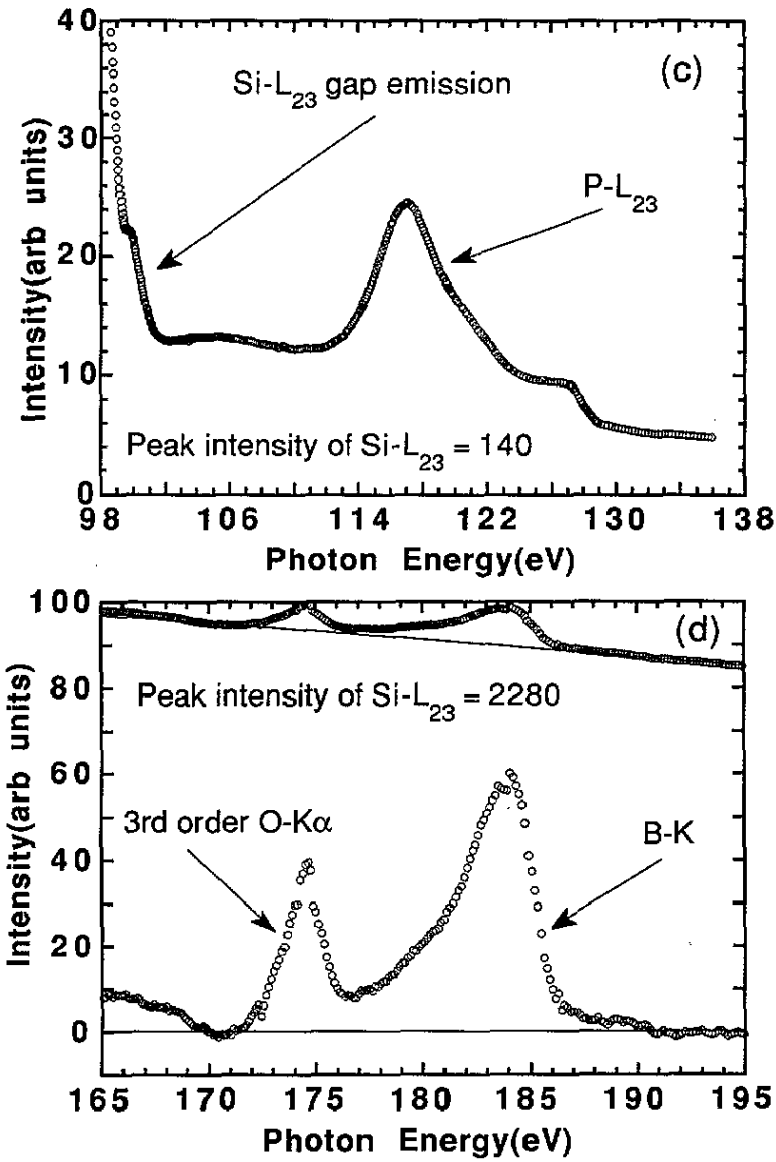

Figure 7. (Continued)

are confined to the first 20 or so Ångstroms from the surface). They would, however, be detected in SXS, which averages over several hundred layers in which defect and H-derived states could form properly, and in which the probabilities of transitions from s-like states to p-like core states are enhanced. Taking the case of SiH_3 groups, there are three nearest-neighbour H atoms to the Si atom whose core levels have been shifted by approximately 1 eV to higher binding energies. The presence of the shift shows that the overlap with H is significant. Hence there can be cross transitions from the three H 2s-derived states to the Si 2p states, resulting in the H 2s half-eV-wide band appearing at about 1 eV above the normal valence band emission edge, as seen in figure 4. The band may show some splitting due to the spin–orbit split core levels. Note that cross transitions of the type discussed here have been observed previously

by Marshall *et al* (1969) and Norris *et al* (1973).

This hypothesis accounts for the dip in the gap state emission previously referred to, since one is observing a separate narrow peak shifted out of the valence band emission. The transitions from Si valence states to the shifted core states compete with the process, but are weakest for Si atoms with the most H neighbours, i.e. SiH_3 groups, which concomitantly show the most core shift and most cross transitions. Hence we interpret the clear peak in figure 4 at 99.8 eV as being due to SiH_3 groups. Their concentration was estimated by Ley *et al* to be 4% of all Si atoms for the surface regions of their ASIL films made by sputtering. In our films made by RF glow discharge, the H concentration was in the region of 15% of which perhaps a quarter was incorporated as SiH_3. There is thus ample amount to account for the observed intensities.

In the case of poorer quality films, as some of those in the series produced by Terekhov *et al* (referred to previously) the gap state tail is larger and shows no dip. This is explained by a greater relative proportion of SiH and SiH_2 groups which have less core shift (the shift is 340 meV per H atom) and greater involvement of Si–Si transitions. They thus smear out the tail and submerge the small sharp peak from the SiH_3 emission.

3.3. Detection of impurity atoms

For direct detection of dopant atoms in ASIL, various techniques are available. Here we report the SXS spectra from both phosphorus and boron in the doped ASIL films, shown in figure 7.

The emission due to transitions to phosphorus L_{23} core holes is clearly evident at 117 eV from the 20% PH_3:SiH_4 film, figure 7(*a*) and (*c*), and is still readily detectable in the 1% PH_3:SiH_4 film, figure 7(*b*). (The feature at 105 eV is the satellite due to doubly ionized Si-L_{23} transitions (Kurmaev and Wiech 1985, Hansen and Arakawa 1972).) The quantitative amounts are of interest, but determination of this is complicated by self-absorption of the radiation by the silicon and by the different ionization cross sections for Si and P L_{23} core levels. Scaling the peak areas from the known peak intensities of Si and P bands, the uncorrected ratio of Si to P peaks was 4.9 for the 20% film and 35.2 for the 1% film. By comparison, an EDAX analysis gave average ratios of Si to P of 2.5 and 19.9 respectively, using only internal program calibrations. The ratio of the two figures, which is more reliable than their absolute values, is 8, which is close to the SXS value of 7.2. (The absolute SXS Si:P ratios seem to be more in accord with expected dopant incorporation than the uncalibrated EDAX figures.) The efficiency of dopant atom incorporation, not to be confused with doping efficiency, varies widely with system parameters but is usually in the range $C_s = C_g^n$, where C_s is concentration in the solid film, C_g is concentration in the gas phase, and n varies from 0.5 to 1 (Szydlo *et al* 1982, Stutzmann *et al* 1987).) From our SXS data we obtain $n = 0.66$. The gas incorporation efficiency has, to our knowledge, not previously been tested to such high dopant concentrations. It is not possible to draw conclusions about the ratio of substitutional-to-interstitial P incorporation as the band is too broad. It is, however, interesting to note that even though the P content of the 20% film is perhaps as high as a few percent, the valence band is not noticeably different from that of the intrinsic film. This indicates that most of the P is incorporated interstitially.

Figure 7(*d*) shows emission due to transitions to boron K core holes, with a peak at 184 eV. The intensity of this emission is much weaker than that from the phosphorus. The ratio of the area under the Si-L_{23} peak to the boron K area is 850:1 to within a

factor of about 2 or better, although again the true ratio would need correction due to absorption and ionization cross section effects. Since the nominal gas ratio was B_2H_6:$SiH_4 = 0.0075$, the data suggest that the B incorporation efficiency is much less than for P, assuming similar transition probabilities. However, this may not be the case. The probability of transition to a boron K hole compared with that to a Si-L_{23} hole is not known, nor are the local density of states factors at B and P sites. When these become known these data will be useful for direct doping comparisons.

4. Conclusion

Analysis of soft x-ray emission spectra from various crystalline and hydrogenated amorphous silicon specimens has shown that boron doped ASIL shows significant differences in the sensitive high-energy part of the valence band emission, compared with intrinsic on phosphorus doped material. This is ascribed to the greater prevalence of direct bonding with hydrogen. The comparatively strong emission observed from the energy gap region is ascribed to cross transitions from nearest-neighbour hydrogen states to shifted core states of silicon. Beam-induced defect states are not involved. Impurity B and P atoms were directly detected, providing information about incorporated densities at high doping levels.

Acknowledgments

We thank V Chacorn and D H Zhang for ASIL film production. This work was supported at University of New South Wales and University of Western Australia by the Australian Research Committee.

References

Allan D C and Joannopoulos J D 1980 *Phys. Rev. Lett.* **44** 43
Carson R D and Schnatterly S E 1987 *Phys. Rev. Lett.* **59** 319
Ching W Y, Lam D J and Lin C C 1979 *Phys. Rev. Lett.* **42** 805
Crisp R S, Haneman D and Chacorn V 1988 *J. Phys. C: Solid State Phys.* **21** 975
Hanson W F and Arakawa E T 1972 *Z. Phys.* **25** 271
Klima J 1970 *J. Phys. C: Solid State Phys.* **3** 70
Kurmaev E Z and Wiech G 1985 *J. Non-Cryst. Solids* **70** 185
Ley L 1984 *Topics in Applied Physics* vol 56, ed J D Joannopoulos and G Lucovsky (Berlin: Springer) ch 3, p 61
Ley L, Reichardt J and Johnson R L 1982 *Phys. Rev. Lett.* **49** 1664
Marshall C A W, Watson L M, Lindsay G M, Rooke G A and Fabian D J 1969 *Phys. Lett.* **28A** 579
Norris P R, Crisp R S and Dimond R K 1973 *Band Structure Spectroscopy of Metals and Alloys* ed D J Fabian and L M Watson (London: Academic) p 229
Ready S E and Boyce J B 1987 *Mat. Res. Soc. Symp. Proc. (USA)* **95** 153
Reimer J A, Vaughan R W and Knights J C 1981 *Phys. Rev.* B **24** 3360
Schneider U and Schröder B 1988 *Amorphous Silicon and Related Materials* ed H Fritzsche (Singapore: World Scientific) p 687
Senemaud C, Pitault B and Bourdon B 1982 *Solid State Commun.* **43** 483
Stutzmann M, Biegelsen D K and Street R A 1987 *Phys. Rev.* B **35** 5666
Suzdlo N, Magarino J and Kaplan D 1982 *J. Appl. Phys.* **53** 5044
Terekhov V A, Golikova O A, Domashevskaya E P, Trostyanskii S N, Mezdrogina M M and Sorokina K L 1984 *Sov. Phys.-Semicond.* **18** 1184

Terekhov V A, Trostyanskii S N, Domashevskaya E P, Golikova O A, Mezdrogina M M, Sorokina K L and Kazanin M M 1986 *Phys. Status Solidi* **138** 674

Wesner D and Eberhardt W 1983 *Phys. Rev.* B **28** 7087

Winer K and Ley L 1988 *Amorphous Silicon and Related Materials* ed H Fritzsche (Singapore: World Scientific) p 365

Yamasaki S, Matsuda A and Tanaka K 1982 *Japan. J. Appl. Phys.* **21** L789